Hindawi
Journal of Nanomaterials
Volume 2018, Article ID 1781389, 8 pages
https://doi.org/10.1155/2018/1781389

Research Article

Single-Photon-Single-Electron Transition for Interpretation of Optical Spectra of Nonspherical Metal Nanoparticles in Aqueous Colloidal Solutions

J. Michael Köhler,[1] Danja Kuhfuß,[1] Phillip Witthöft,[2] Martina Hentschel,[3] and Andrea Knauer[1]

[1]*Institute for Micro- und Nanotechnologies/Institute for Chemistry and Biotechnology, Department of Physical Chemistry and Microreaction Technology, Technische Universität Ilmenau, 98693 Ilmenau, Germany*
[2]*MIN Fakultät, Institute of Physical Chemistry, Universität Hamburg, Grindelallee 117, 20146 Hamburg, Germany*
[3]*Institute for Micro- und Nanotechnologies/Institute for Physics, Department of Theoretical Physics II/Computational Physics, Technische Universität Ilmenau, 98693 Ilmenau, Germany*

Correspondence should be addressed to Andrea Knauer; andrea.knauer@tu-ilmenau.de

Received 30 April 2018; Revised 2 August 2018; Accepted 7 August 2018; Published 30 August 2018

Academic Editor: Rajesh R. Naik

Noble metal nanoparticles—especially shape anisotropic particles—have pronounced resonances in the optical spectrum. These sensitive absorption modes attract great interest in various fields of application. For nonspherical particles, no analytic description of the absorption spectra according to the commonly used Mie theory is possible. In this work, we present a semi-empirical approach for the explanation of the optical spectra of shape anisotropic particles such as silver nanoprisms and gold nanorods. We found an interpretation of the optical absorption spectra which is based on a single-photon-single-electron transition. This model is in a better agreement with the basic assumptions of quantum mechanics than the electrodynamic model of a localized surface plasmon excitation. Based on microfluidically obtained Ag nanoprisms and Au nanorods with very high ensemble homogeneities, dependencies between the geometrical properties of the shape anisotropic noble metal nanoparticles and the spectral position of the longitudinal absorption mode could be derived, which show that the assumption of a composed relative permittivity and the inclusion of the Rydberg constant is sufficient to describe the optical properties of the shape anisotropic particles. Within the scope of the measuring accuracy, the calculations furthermore lead to the value of the refractive index of the particle-surrounding medium.

1. Introduction

The optical spectra of metal nanoparticles are mostly interpreted by the assumption of the excitation of plasmons [1]. This interpretation has caused the frequent use of the terminus "particle plasmonics" for the investigation and application of metal nanoparticles with characteristic electromagnetic resonances [2]. This interpretation uses the classical theory of electromagnetism and the explanation of Mie for the light scattering and absorption of single or dispersed spherical metal nanoparticles [3]. This model supplied precise optical data for spherical particles [4], but it is not easy to apply it to particles of lower symmetry, in particular for nonspherical particles like rods, disks, or flat prisms [2, 5–7]. But the optical resonances of these particles are particularly interesting and strongly related to their size and geometry. In addition, it was found that the resonances are dependent on the chemical environment, the surface functionalization [8], and electrical charging of particles [9], which makes them very attractive for new analytical and labelling methods [6, 10–12].

The plasmon model is based on the idea of a field-induced collective oscillation of electrons. Analogue elongation and relaxation of all electrons always take place if

photons pass matter, and this simple response on the electromagnetic field is the general cause for the effect of light refraction by elastic interaction between photons and matter. Nonelastic interactions are marked by a nonreversible energy transfer between the electromagnetic field and the energy-absorbing material. The electromagnetic resonances of atoms and molecules are well understood by quantum mechanics using the model of atom or molecule orbitals. They can be explained by one-photon-one-electron processes, typically [13, 14].

Nonspherical particles have to be regarded as dimension-reduced systems, if their geometries are marked by higher aspect ratios. This means that these particles could be regarded in analogy to small compact solids in one or two directions, but they have to be regarded in analogy to clusters or molecules in the other directions. Nanorods are "one-dimensional" objects, which means they are size-reduced in two dimensions. Flat nanodisks or prisms are two-dimensional objects with a size reduction in one dimension. Therefore, their resonance behaviour can hardly be understood by models presuming a spherical symmetry. In particular, it has to be taken in mind that the reduction in dimension can cause special functions of state densities for the possible energy levels as it is known from molecular objects. Thus, the transfer of energy from the electromagnetic field into electronic states of the shape-anisotropic metal nanoparticles should be related to the electronic state distribution and the transfer of a single electron from a lower to higher energetic level.

Lower yields in the many syntheses of special nanoparticle types and larger distributions in shape and size of these particles prevented a detailed interpretation of the measured electromagnetic resonances of nonspherical particles by an excitation model. A better precondition for understanding of the optical properties came from single-particle investigations [15–17]. These investigations are typically related to particles deposited on a surface, and the investigation methods are difficult to transfer to colloidal solutions.

Next to metallic particles that show pronounced absorption in the visible range and the near UV, also charged and uncharged dielectric particles such as water, ice, and cosmic dust have already been investigated regarding the interaction between electrical charges and electromagnetic radiation. Here, it was found by Kocifaj et al. that the long-wavelength resonances in the optical spectra are an effect of excess surface charges. The physical behaviour of the net charges is related to a surface current density, which shows a linear dependence to a phenomenological surface conductivity [18]. Furthermore, it was shown from the same authors that, in the case of the mentioned nonconductive particles, the resonant wavelength is 100–1000 times larger than the characteristic size of the investigated nanoparticles [19].

For especially noble metal nanoparticles, new synthesis methods, in particular microfluidic syntheses, allow the generation of dispersed metal nanoparticles in colloidal solution with high yield and very small distribution in size and geometry [20–22]. The products of these syntheses can be regarded as homogeneous—approximately comparable to the identity of the particles of a single molecular substance. This opens the possibility to investigate the electronic properties of nanoparticles in ensembles in colloidal solutions in analogy to the investigation of pure molecular substances in solutions. In the following, the spectrophotometric investigation of such colloidal product solutions of flat silver nanoprisms and gold nanorods of different sizes and aspect ratios is used for the interpretation of their resonance behaviour by one-photon-one-electron excitation processes.

2. Experimental

2.1. Microfluidic Arrangements for Nanoparticle Synthesis. For the microfluidic synthesis of Au nanorods as well as for Ag nanoprisms, modular reactors were designed. The reactor channels are PTFE tubes with an inner diameter of 0.5 mm. The tubing is connected to glass syringes (ILS, Ilmenau, Germany) in syringe pumps (Cetoni neMESYS, Cetoni GmbH) with standard fluid connectors, which are commercially available as HPLC equipment (IDEX Health & Science, LCC). A schematic illustration of an exemplary reactor for the synthesis of Au nanorods is shown in Figure 1. The micro flow-through synthesis of silver nanoprisms has been explained in detail before [23].

2.2. Batch Synthesis of Au Nanorods with Higher Aspect Ratios. Au nanorod samples were prepared by two different synthesis pathways. Using the synthesis developed by Ye et al. [24], eleven Au nanorod batches with diameters above 10 nm and different aspect ratios between 2 and 8 have been produced. Furthermore, by exploiting the synthesis route developed by Jia et al. [25], five batches of smaller Au nanorods with diameters smaller than 6 nm and aspect ratio between 2 and 4 have been prepared. Mean values for the dimensions of the nanorods, in particular their aspect ratio, have been obtained by evaluating TEM images and averaging at least 200 particles of each batch.

Both synthesis strategies base on seeded growth approaches via chloroauric acid reduction in aqueous solution. Sodium borohydride reduces tetrachloroauric acid in the seed solution to elementary gold and induces nucleation whereas tetrachloroauric acid in the growth solution is reduced with ascorbic acid only to an oxidation state of +I [26]. By mixing both solutions, the seed surfaces act as catalysts for the final reduction step and the following particle growth.

2.3. Nanoparticle Characterization. The colloidal solutions of the obtained nobel metal nanoparticles were analyzed using UV-vis spectrophotometry (SPECORD 200 Analytik Jena/Cary 5000 UV-Vis-NIR spectrophotometer), SEM (Hitachi S-4800, FE-SEM), TEM (Philips CM 300), and DCS measurement for the knowledge of the differential size distribution spectra of the Stokes equivalent sedimentation diameter (DCS, DC 20000, CPS Instruments, Inc.).

2.4. Chemicals and Materials. All chemicals used for the synthesis of Au nanorods or Ag nanoprisms were used as received from the following suppliers (purity of chemicals in brackets): sodium citrate (Merck KGaA, 99%), poly(sodium

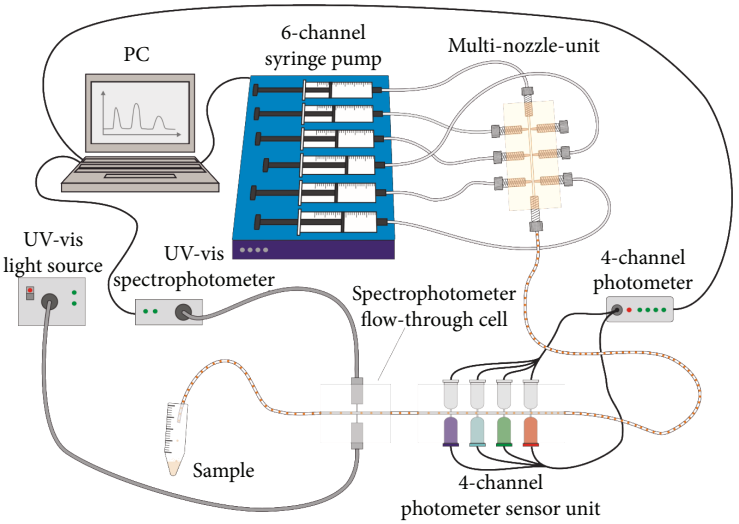

Figure 1: Exemplary sketch of a modular microflow-through reactor which is operated in a segmented flow mode. The carrier stream of an organic, immiscible liquid phase (e.g., longer alkanes or perfluorinated alkanes) is presented first in a continuous stream. Into the carrier stream, aqueous reactant solutions are dosed under simultaneous formation of aqueous droplets. These aqueous droplets can be considered as closed-up microbatch reactors with efficient droplet internal mixing conditions.

styrenesulphonate) (PSS) (Acros Organics, M_W: 70 or 100 kDa), sodium borohydride (Merck KGaA, 99%), silver nitrate (Merck KGaA, 99%), ascorbic acid (Merck KGaA, 99.7%), cetyltrimethylammonium bromide (Merck KGaA, 99%), tetrachloroaurate(III) hydrate (Carl Roth GmbH & Co. KG, >99.5%). Perfluoromethyldecalin (F2 Chemicals Ltd) was used in both syntheses as carrier medium to achieve a segmented flow. All solutions were prepared in ultrapure, particle-filtered water. The specific electric resistivity of the used water was 18.2 MΩ·cm. All experiments were carried out under clean-room conditions.

3. Description of Electromagnetic Resonances

3.1. One-Photon-One-Electron Approach. The following approach is based on the idea that the electronic excitation of so-called plasmonic particles has to be understood in analogy to the electronic excitation of molecules. From the classical view of Coulomb's law, the energy of an electrostatic field is determined from the ratio of the square of separated charges Q and the distance between them r. Certain electrical field energy can be described either by a high charge in a long distance or by a lower charge in a short distance. Similarly, the energy of an oscillating electrical field can be described either by a high number of electrons moving with low amplitude or by the oscillation of a low number of electrons with higher amplitude.

In contrast to the classical approach, quantum mechanics is strongly particle-related. The resonant interaction of atoms and molecules with the electromagnetic field is always a process of interaction between a small number of atoms and molecules and a small number of resonant photons, typically an excitation (absorption) or emission (fluorescence) event in form of a one-photon-one-electron process.

It is assumed that the so-called plasmonic particle excitation is also a resonant one-photon-one-electron process. The resonant transition is controlled by energy eigenstates of the particle which is strongly related to the particle geometry. The involved states can be regarded in analogy to the extended pi orbitals of a dye molecule containing a chain of conjugated double bonds.

For the approximation of the resonance energy, it is assumed that the energy of absorbed photon with the wavelength λ is equal to the electrostatic energy of one excited electron with the charge q_e in a metal nanoparticle with a linear extension of L

$$h * \frac{c}{\lambda} = \frac{q_e^2}{4\pi * \varepsilon_0 * \varepsilon_r * L}. \quad (1)$$

The electrical field constant ε_0 can be expressed by the fine structure constant (FSK) α

$$\varepsilon_0 = \frac{{q_e}^2}{2h * c * \alpha}. \quad (2)$$

This results into the simple expression for the resonance wavelength:

$$\lambda = \frac{2\pi}{\alpha * \varepsilon_r * L}. \quad (3)$$

It is further assumed that ε_r can be expressed by the sum of a metal-related term with the parameter a_{met} and an environment-related term containing a parameter b_{env} describing the environment of the particle (L is the length or the lateral extension of the nanoparticles)

$$\varepsilon_r = \frac{a_{met}}{L} + b_{env} * \frac{\alpha}{2\pi}. \quad (4)$$

3.2. Approximation of Resonance Wavelengths for Nanotriangles and Nanorods. The resonance wavelength of triangles was approximated by using (3) and (4):

$$\lambda_{\text{triangles}} = \frac{2\pi}{\alpha} * L * \left(\frac{a_{\text{met}}}{L} + b_{\text{env,triangle}} * \frac{\alpha}{2\pi}\right), \quad (5)$$

$$\lambda_{\text{triangles}} = \frac{2\pi}{\alpha} * a_{\text{met}} + b_{\text{env,triangle}} * L. \quad (6)$$

This equation corresponds to the empirically found linear equation for the dependence of the resonance wavelength of triangles from their lateral size [27].

The resonance wavelength for nanorods can be approximated in complete analogy to the flat nanotriangles (5 and 6). The only difference exists in the different parameter b, which depends on the particle geometry:

$$\lambda_{\text{rod}} = \frac{2\pi}{\alpha} * L * \left(\frac{a_{\text{met}}}{L} + b_{\text{env,rod}} * \frac{\alpha}{2\pi}\right), \quad (7)$$

$$\lambda_{\text{rod}} = \frac{2\pi}{\alpha} * a_{\text{met}} + L * b_{\text{env,rod}}. \quad (8)$$

4. Experimental Results and Discussions

4.1. Nanoparticle Synthesis. The investigations of Aherne and coworkers [28] have shown how to precisely tune the nanoprism's edge length by shifting the ratio of seeds and silver nitrate for the particle growth reaction. This approach was also applied for the microflow synthesis. The seed nanoparticle density was varied in the reaction solution while keeping the concentration of the metal salt ($AgNO_3$) constant [23]. It is reflected in the optical spectra of the product samples (Figure 2) that a higher amount of seed particles leads towards smaller silver nanoprisms and a decreasing amount of silver seed particles will lead towards larger silver nanoprisms. Using microfluidic syntheses, a precise tuning of the prism's edge length is possible and thus also an exact adjustment of the spectral position of the longitudinal absorption mode.

With the flow-through synthesis of gold nanorods, a precise tuning of the physical properties by shifting the crucial reactant ratios succeeded as well. SEM images of microflow-produced Ag nanoprisms of two different sizes are exemplarily shown in Figures 3(a) and 3(b).

In experiments with different seed nanoparticle densities, Au of aspect ratios between 2.4 and 3.8 has been obtained. It was found that the seed concentration is mainly influencing the final diameters of the nanorods, whereas the effect of a varying seed particle density on the nanorod's length is less distinct. A low seed particle density leads towards slightly longer but significantly thicker rods, while from a high amount of seed nanoparticles much thinner but little shorter rods were obtained. The shift in the aspect ratio and particle size is directly connected with the change in the optical absorption spectra. Here, a red shift of the spectral position of the long-wavelength absorption results, if the seed particle concentration is enhanced. At lower seed concentrations, the absorption peak is shifted hypsochromically.

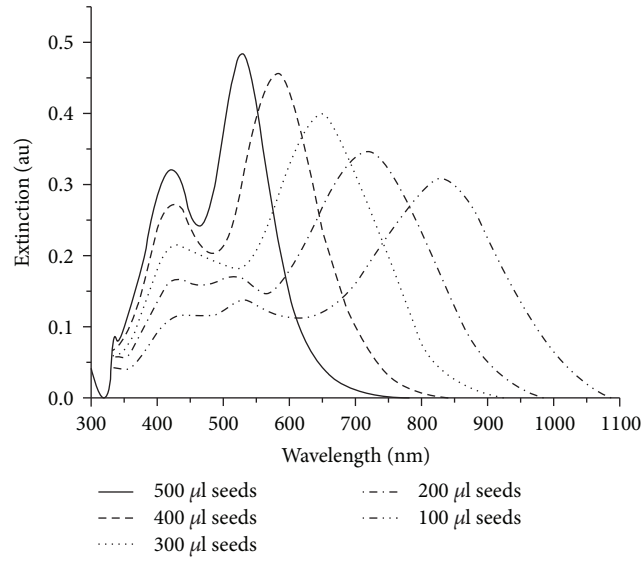

Figure 2: UV-vis spectra of five silver nanoprism samples with different particle sizes each. The spectral position of the main absorption mode is shifted bathochromically with a larger edge length, which were obtained under conditions of decreasing seed nanoparticle density [21].

Additionally, an increase in the extinction of the shorter-wavelength resonance mode is observed (Figure 4). This indicates an increase in the excitation probability in direction of the short axes of the nanorods, which can be drawn back to the increase in the rod diameter and the associated decrease in the aspect ratio.

Au nanorods with higher aspect ratios produced in wet chemical approaches show diameters between 5 nm and 30 nm with aspect ratios between 2 and 8. The spectral positions of the longitudinal absorption modes vary in the range of 700 nm to 1200 nm.

Au nanorods with tailor-made aspect ratios and adjustable longitudinal absorption modes have been synthesized by varying the amount of seed solution, the amount of ligands in the reaction solution, and the pH value, if all other conditions remain constant. By increasing the amount of seed solution, Au nanorods became thinner on average, which results in an increased aspect ratio due to less available gold per Au nanorod and a faster growth process in the longitudinal direction. The same result can be observed by increasing the amount of ligands due to earlier saturation of the Au nanorod surfaces as well as reducing the pH value by increasing the amount of hydrochloric acid. This effect can be attributed to different micelle stabilities of the CTAB micelles at different pH values [29]. SEM images of Au rods with lower and larger aspect ratios are shown in Figures 5(a) and 5(b).

4.2. Geometry-Dependent Resonances of Colloidal Solutions. The application of (6) for the interpretation of the dependence of the long-wavelength resonance from the particle size leads to a constant first term of about 500 nm. This number is valid for nanorods as well as for nanotriangles. It can be interpreted as the resonance of a small compact particle. It

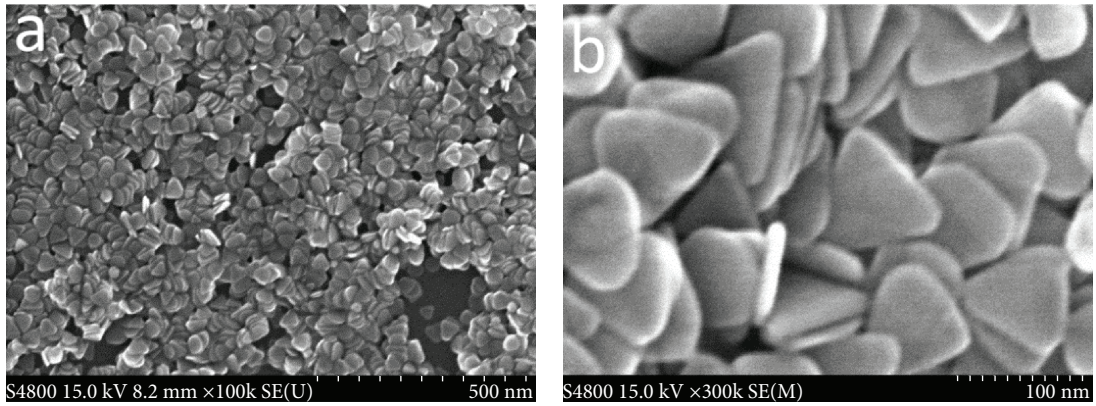

(a) (b)

Figure 3: (a and b) SEM images of (a) Ag nanoprisms with about 35 nm edge length and (b) Ag prisms with about 120 nm edge length.

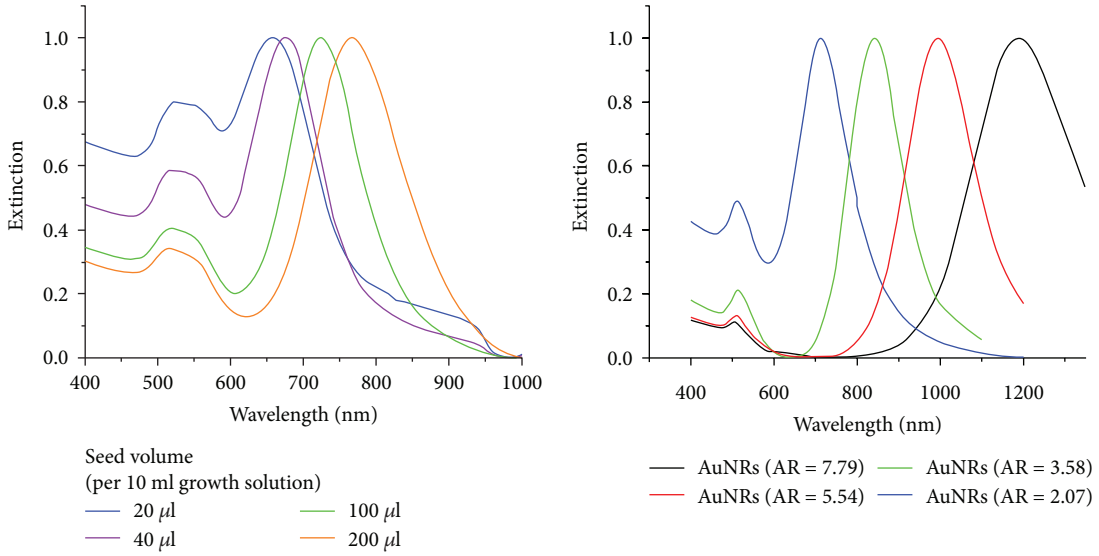

(a) (b)

Figure 4: (a) Optical absorption spectra of Au nanorods. Here, an increasing seed volume leads towards a red shift of the main absorption mode. With increasing seed particle density, the aspect ratio of the rods increases, not the rod length. Rods prepared under conditions of high seed particle densities are slightly shorter but markedly thinner. (b) UV-Vis spectra of Au nanorods with aspect ratios between 2.07 and 7.79.

agrees with the resonance wavelength of small spherical gold nanoparticles, in first approximation.

The parameter $b_{\text{env,triangle}}$ can be identified with the square of the refractive index of the surrounding medium for $n_{\text{env}} = 1.36$. Figure 6 shows the correlation of the experimental results with this interpretation.

$$\lambda_{\text{triangle}} = \frac{2\pi}{\alpha} * a_{(\text{Ag})} + L * {n_{\text{env}}}^2. \tag{9}$$

The approximation of the experimental data supplies

$$\frac{2\pi}{\alpha} * a_{(\text{Ag})} \approx 482\,\text{nm} \approx 490\,\text{nm}, \tag{10}$$

$$\lambda_{\text{triangle}} = 482\,\text{nm} + L * 1.36^2. \tag{11}$$

The experimental data for the gold nanorods suggest that the parameter $b_{\text{env,rod}}$ can be described in dependence of the aspect ratio f and the refractive index of the surrounding medium n_{env}. The experimental results can be approximated by the following empirical linear relation

$$\lambda_{\text{rod}} = n + m * (f - 1). \tag{12}$$

It was found that the remaining factor is nearly identical with the ratio of the inverse Rydberg constant R_{oo} and the rod length

$$b_{\text{env,rod}} = (f - 1) * n_{\text{env}} * \frac{(1/R_{oo})}{L}. \tag{13}$$

The experimental data show a good agreement between the expected refractive index (corresponding to (9)) and the

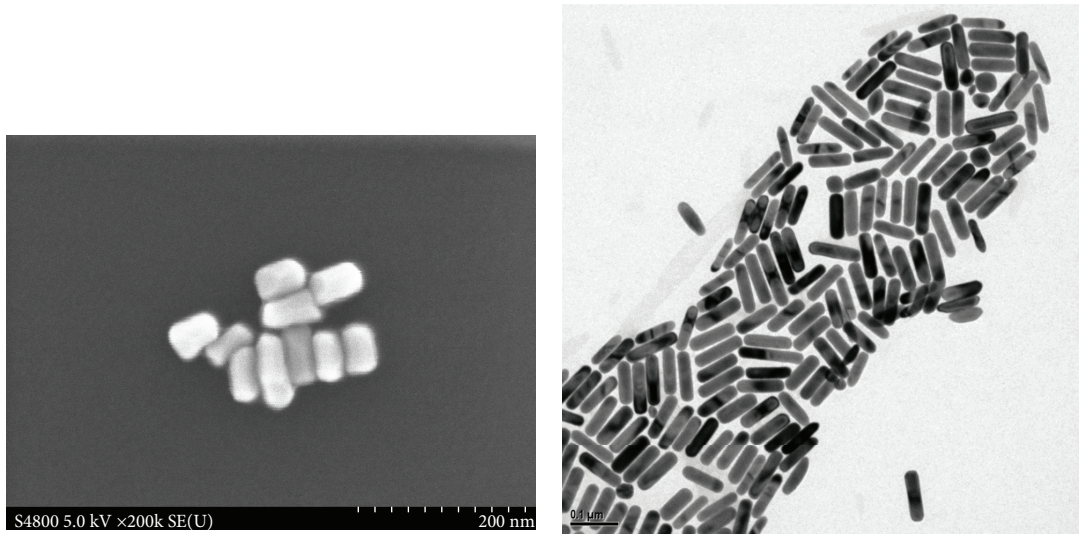

(a) (b)

Figure 5: (a and b) Electron microscope images of (a) (SEM) Au nanorods with small aspect ratio (SEM) and (b) larger aspect ratio (TEM).

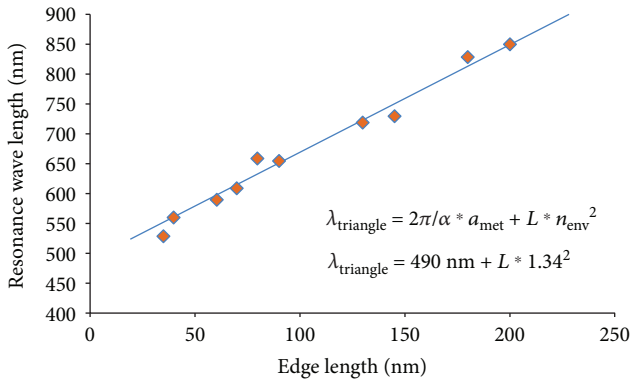

Figure 6: Correlation between the spectral position of the main resonance wavelengths of silver nanoprism solutions and the SEM-determined average edge length of the individual prism samples.

value obtained from different nanorod syntheses in aqueous solution. The resonance wavelength of nanorods can be approximated by the following version of (8):

$$\lambda_{rod} = \frac{2\pi}{\alpha} * a_{(Au\text{-}rod)} + (f-1) * n_{env} * \left(\frac{1}{R_{oo}}\right). \quad (14)$$

$$\lambda_{rod} = 490\ nm + (f-1) * 1.34 * \left(\frac{1}{R_{oo}}\right). \quad (15)$$

The approximation of Figure 7 is given by the following parameters:

$$\frac{2\pi}{\alpha} * a_{met} = 490\ nm, \quad (16)$$

$$n_{env} = 1.34. \quad (17)$$

The parameter a_{met} ($a_{(Ag)}$, $a_{(Au-rod)}$) can be interpreted as a reference length l_0, which can be derived from (11) and (16):

$$a_{met} = l_0 \approx 490\ nm * \frac{\alpha}{2\pi} \approx 0.57\ nm. \quad (18)$$

This value can be approximated by

$$a_{met} = l_0 \approx 0.856 * \frac{a}{R_{oo}}. \quad (19)$$

It seems that this reference length is significantly dependent neither on the metal nor on the geometry of nanoparticles, but mainly defined by the fine structure constant α and the Rydberg constant R_{oo}.

The approximation of the axial resonance wavelength of gold nanorods in dependence on the aspect ratio f can then be expressed by

$$\lambda_{rod} = \left(\frac{1}{R_{oo}}\right) * [5.38\ nm + (f-1) * n_{env}]. \quad (20)$$

5. Conclusions

New microfluidic and batch syntheses generate gold nanorods and flat triangular silver nanoprisms with very high yields and high homogeneities, whereby the particles have been obtained dispersed in colloidal aqueous solution. The narrow distribution of size and shape and the possibility of tuning the extension of particles allowed obtaining well reproducible data of the long-wavelength electromagnetic resonances.

It was found that the dependence of the resonance wavelength on the particle size can be interpreted in case of both particle types by a one-photon-one-electron excitation process, which is in better agreement with the basic assumptions

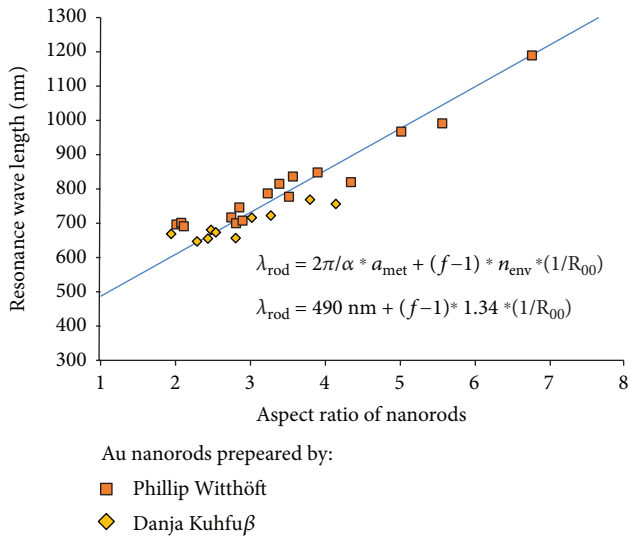

FIGURE 7: Dependence between the axial absorption maximum of gold nanorods and their SEM-determined aspect ratio.

of quantum mechanics than the classical model of a particle plasmon excitation. The linear approximation led to an interpretation using an ε_r, which is composed of a metal-related and an environmentally related part. Both parts can be approximated by the characteristic geometry parameters and fundamental constants and yield the refractive index of the particle-surrounding liquid medium.

Data Availability

The UV-Vis, SEM, and TEM data used to support the findings of this study are available from the corresponding author upon request.

Conflicts of Interest

There are no conflicts of interest to declare.

Acknowledgments

The authors gratefully acknowledge the financial support from the DFG (KO 1403/39-1 and HE 3494/3, Emmy Noether Program). The work of Phillip Witthöft is funded by a scholarship from the PIER Helmholtz Graduate School.

References

[1] U. Kreibig and M. Vollmer, *Optical Properties of Metal Clusters*, Springer-Verlag Berlin Heidelberg, Berlin, Heidelberg, 1995.

[2] S. Link and M. A. El-Sayed, "Spectral properties and relaxation dynamics of surface plasmon electronic oscillations in gold and silver nanodots and nanorods," *Journal of Physical Chemistry B*, vol. 103, no. 40, pp. 8410–8426, 1999.

[3] G. Mie, "Beiträge zur Optik trüber Medien, speziell kolloidaler Metallösungen," *Annalen der Physik*, vol. 330, no. 3, pp. 377–445, 1908.

[4] M. Quinten, *Optical Properties of Nanoparticle Systems - Mie and Beyond*, Wiley-VCH Verlag & Co. KGaA, 2011.

[5] N. Large, J. Aizpurua, V. K. Lin et al., "Plasmonic properties of gold ring-disk nano-resonators: fine shape details matter," *Optics Express*, vol. 19, no. 6, pp. 5587–5595, 2011.

[6] E. Cubukcu, Nanfang Yu, E. J. Smythe, L. Diehl, K. B. Crozier, and F. Capasso, "Plasmonic laser antennas and related devices," *IEEE Journal of Selected Topics in Quantum Electronics*, vol. 14, no. 6, pp. 1448–1461, 2008.

[7] W.-Y. Chien and T. Szkopek, "Multiple-multipole simulation of optical nearfields in discrete metal nanosphere assemblies," *Optics Express*, vol. 16, no. 3, 2008.

[8] S. Takae, Y. Akiyama, H. Otsuka, T. Nakamura, Y. Nagasaki, and K. Kataoka, "Ligand density effect on biorecognition by PEGylated gold nanoparticles: regulated interaction of RCA_{120} lectin with lactose installed to the distal end of tethered PEG strands on gold surface," *Biomacromolecules*, vol. 6, no. 2, pp. 818–824, 2005.

[9] S. K. Dondapati, M. Ludemann, R. Muller et al., "Voltage-induced adsorbate damping of single gold nanorod plasmons in aqueous solution," *Nano Letters*, vol. 12, no. 3, pp. 1247–1252, 2012.

[10] A. Csaki, R. Möller, W. Straube, J. M. Köhler, and W. Fritzsche, "DNA monolayer on gold substrates characterized by nanoparticle labeling and scanning force microscopy," *Nucleic Acids Research*, vol. 29, no. 16, article e81, 2001.

[11] K. Liszewski, "Applying nanoparticles as molecular tags - fundamental shift in biological labeling," *Genetic Engineering News*, vol. 21, no. 9, 2001.

[12] H. L. Wu, H. R. Tsai, Y. T. Hung et al., "A comparative study of gold nanocubes, octahedra, and rhombic dodecahedra as highly sensitive SERS substrates," *Inorganic Chemistry*, vol. 50, no. 17, pp. 8106–8111, 2011.

[13] R. E. Palmer, "Electron-molecule dynamics at surfaces," *Progress in Surface Science*, vol. 41, no. 1, pp. 51–108, 1992.

[14] W. F. Chan, G. Cooper, and C. E. Brion, "Absolute optical oscillator strengths for the electronic excitation of atoms at high resolution: experimental methods and measurements for helium," *Physical Review A*, vol. 44, no. 1, pp. 186–204, 1991.

[15] T. Sannomiya, C. Hafner, and J. Voros, "Shape-dependent sensitivity of single plasmonic nanoparticles for biosensing," *Journal of Biomedical Optics*, vol. 14, no. 6, p. 064027, 2009.

[16] E. Ringe, J. M. McMahon, K. Sohn et al., "Unraveling the effects of size, composition, and substrate on the localized surface plasmon resonance frequencies of gold and silver nanocubes: a systematic single-particle approach," *Journal of Physical Chemistry C*, vol. 114, no. 29, pp. 12511–12516, 2010.

[17] W. S. Hwang, P. L. Truong, and S. J. Sim, "Size-dependent plasmonic responses of single gold nanoparticles for analysis of biorecognition," *Analytical Biochemistry*, vol. 421, no. 1, pp. 213–218, 2012.

[18] M. Kocifaj, J. Klačka, F. Kundracik, and G. Videen, "Charge-induced electromagnetic resonances in nanoparticles," *Annalen der Physik*, vol. 527, no. 11-12, pp. 765–769, 2015.

[19] J. Klačka and M. Kocifaj, "Scattering of electromagnetic waves by charged spheres and some physical consequences," *Journal of Quantitative Spectroscopy and Radiative Transfer*, vol. 106, no. 1-3, pp. 170–183, 2007.

[20] J. Boleininger, A. Kurz, V. Reuss, and C. Sonnichsen, "Microfluidic continuous flow synthesis of rod-shaped gold and silver

nanocrystals," *Physical Chemistry Chemical Physics*, vol. 8, no. 33, pp. 3824–3827, 2006.

[21] S. Duraiswamy and S. A. Khan, "Droplet-based microfluidic synthesis of anisotropic metal nanocrystals," *Small*, vol. 5, no. 24, pp. 2828–2834, 2009.

[22] S. Marre and K. F. Jensen, "Synthesis of micro and nanostructures in microfluidic systems," *Chemical Society Reviews*, vol. 39, no. 3, pp. 1183–1202, 2010.

[23] A. Knauer, A. Csaki, F. Moller, C. Huhn, W. Fritzsche, and J. M. Kohler, "Microsegmented flow-through synthesis of silver nanoprisms with exact tunable optical properties," *Journal of Physical Chemistry C*, vol. 116, no. 16, pp. 9251–9258, 2012.

[24] X. Ye, Y. Gao, J. Chen, D. C. Reifsnyder, C. Zheng, and C. B. Murray, "Seeded growth of monodisperse gold nanorods using bromide-free surfactant mixtures," *Nano Letters*, vol. 13, no. 5, pp. 2163–2171, 2013.

[25] H. Jia, C. Fang, X. M. Zhu, Q. Ruan, Y. X. J. Wang, and J. Wang, "Synthesis of absorption-dominant small gold nanorods and their plasmonic properties," *Langmuir*, vol. 31, no. 26, pp. 7418–7426, 2015.

[26] L. Scarabelli, A. Sanchez-Iglesias, J. Perez-Juste, and L. M. Liz-Marzan, "A "tips and tricks" practical guide to the synthesis of gold nanorods," *Journal of Physical Chemistry Letters*, vol. 6, no. 21, pp. 4270–4279, 2015.

[27] A. Knauer and J. M. Koehler, "Explanation of the size dependent in-plane optical resonance of triangular silver nanoprisms," *Physical Chemistry Chemical Physics*, vol. 18, no. 23, pp. 15943–15949, 2016.

[28] D. Aherne, D. M. Ledwith, M. Gara, and J. M. Kelly, "Optical properties and growth aspects of silver nanoprisms produced by a highly reproducible and rapid synthesis at room temperature," *Advanced Functional Materials*, vol. 18, no. 14, pp. 2005–2016, 2008.

[29] J. Cheng, L. Ge, B. Xiong, and Y. He, "Investigation of pH effect on gold nanorod synthesis," *Journal of the Chinese Chemical Society*, vol. 58, no. 6, pp. 822–827, 2011.